

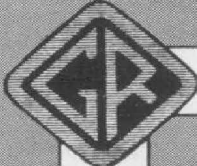
THE

# General Radio EXPERIMENTER

VOLUME XXI No. 8

JANUARY, 1947

Copyright, 1947, General Radio Company, Cambridge, Mass., U. S. A.



ELECTRICAL MEASUREMENTS AND THEIR INDUSTRIAL APPLICATIONS

## GENERAL RADIO ENLARGES PLANT

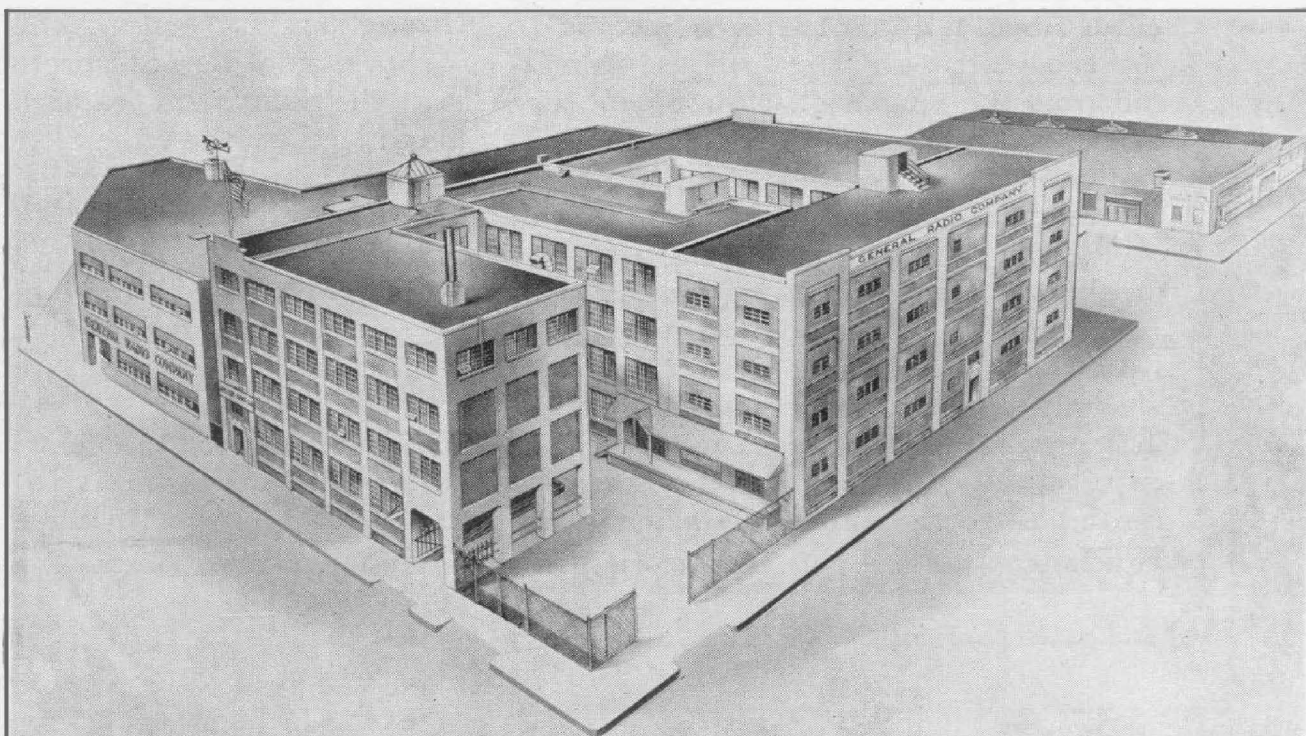
*Also*

### IN THIS ISSUE

	PAGE
THOSE IRON-CORED COILS AGAIN—Part II. FRINGING AT AN AIR GAP.....	2
F.C.C. APPROVAL NUMBERS FOR GENERAL RADIO BROADCAST MONITORS....	8
MISCELLANY .....	8

●**WORK** is progressing on a new four-story addition to the General Radio plant. This new building, located at the corner of State and Windsor Streets, Cambridge, will add approximately 30,000 square feet to the Company's manufacturing space, bringing the total plant space to 145,000 square feet. It will be used to house some of the manufacturing operations now being carried on in rented quarters and will also provide space for an increase in manufacturing capacity.

The accompanying drawing shows the plant as it will appear when construction is completed next summer. The new section is the right-hand unit of the main group.



## THOSE IRON-CORED COILS AGAIN

### PART II

#### FRINGING AT AN AIR GAP

The other improvement made since the March, 1942, article<sup>1</sup> comes in a better understanding of the mechanism which governs the effective permeability of a core of ferro-magnetic material with an air gap in its center leg. Reference was made to uncertainties in this respect at the middle of the text of page 3 and at the end of page 12 of the March, 1942, article. Measurements and calculations made in the meantime have indicated a method that can be used to explain the behavior of measured coils and to forecast the behavior of others.

#### Theory

Equation (3a) on page 8 of the March, 1942, article, which gives the approximate relationship between true and apparent permeability, can be rewritten as follows (where  $\mu_t\alpha \gg 1$ ):

$$\frac{l}{\mu\alpha} = \frac{l}{\mu_t\alpha} + g \quad (29)$$

This equation states that the equivalent air length of the magnetic circuit of any structure, to be used in determining the inductance of a coil thereon, is equal to the equivalent air length of the iron itself plus the length of the air gap. The equivalent air length of the iron, for instance, is equal to the actual length of the flux path in the magnetic material, divided by the product of its true permeability and the stacking factor.

Strictly, the  $l$  in the term  $l/\mu_t\alpha$  of Equation (29) should be written  $(l - g)$  to account for the reduction in path length in magnetic material occasioned by the gap. Actually, the complication is unwarranted, since the difference is negligible.

If Equation (29) is combined with Equation (6)<sup>2</sup> to replace the unknown  $\mu$  by directly measurable  $L$ , the following is obtained:

$$\frac{1}{L} \left( \frac{4\pi N^2 A}{10^9} \right) = \frac{l}{\mu_t\alpha} + g \quad (30)$$

This equation states that if the reciprocal of the measured inductance, multiplied by the proper factor determinable from constants of the structure, be plotted as abscissa against air gap as ordinate, the result should be a straight line inclined upward at 45°. It will not go through the origin, since the value of  $l/\mu_t\alpha$  is finite.

Unfortunately, such a plot is not a straight line having the proper slope. It has approximately the right slope for points with very small ordinates, but soon begins to curve upward away from the 45° line as the ordinates increase. The reason for this will be shown to be the fringing at the air gap, which makes the reluctance of the gap smaller than its measured length would indicate, because of the larger equivalent *area*. Since the simple theory is easier to use if the area of the magnetic circuit is the same throughout its length, this last statement should be interpreted as saying that the equivalent *length* of the air gap is reduced by the effects of the fringing. It would be helpful to be able to calculate simply the effects of fringing.

Before that is gone into, however, one other refinement of the equation should be made. The intercept on the axis of ordinates would, by (30), represent only the value of  $l/\mu_t\alpha$ . Actually it always comes out larger than that value (if  $\mu_t$  is assigned a representative value commonly associated with the magnetic ma-

<sup>1</sup> P. K. McElroy and R. F. Field, "How Good is an Iron-Cored Coil?" *General Radio Experimenter*, March, 1942.

<sup>2</sup> See Part I, December, 1946, *Experimenter*.



terial in use). The difference represents the reluctance of a butt joint in the center leg which can be assigned, for convenience, an equivalent air length.

We then have the following equation, which will yield a straight-line plot:

$$\frac{1}{L} \left( \frac{4\pi N^2 A}{10^9} \right) = g' + b + \frac{l}{\mu_t \alpha} \quad (31)$$

where  $g' =$  equivalent length of measured air gap ( $g' < g$ )

and  $b =$  equivalent air length of butt joint.

Empirical information will be used which has been described in the first part hereof, namely, measurements of inductance against various air gaps. A method will be developed for calculating the effective air gap length. The fact that effective air gap lengths obtained by this method yield fairly good 45° straight lines when plotted will attest to the validity of the method for the purpose.

### Effect of Fringing

This analysis was inspired by Chapter V on "Calculation of the Permeance of Flux Paths through Air between Surfaces of High-Permeability Material," of *Electromagnetic Devices*, by Herbert C. Roters, Wiley, 1941. While the whole chapter is useful in that it establishes a feeling of confidence in the methods Mr. Roters suggests, the meat for the present purpose is encompassed in Section 53 on Special Formulas for Use in the Method of "Estimating the Permeances of Probable Flux Paths." Reference will be made, by the terminology used in that section, to the various probable flux paths used in this calculation.

The conditions obtaining in a typical shell-type-lamination structure where there is an air gap in the center leg are covered by Figures 8 and 17 of Mr.

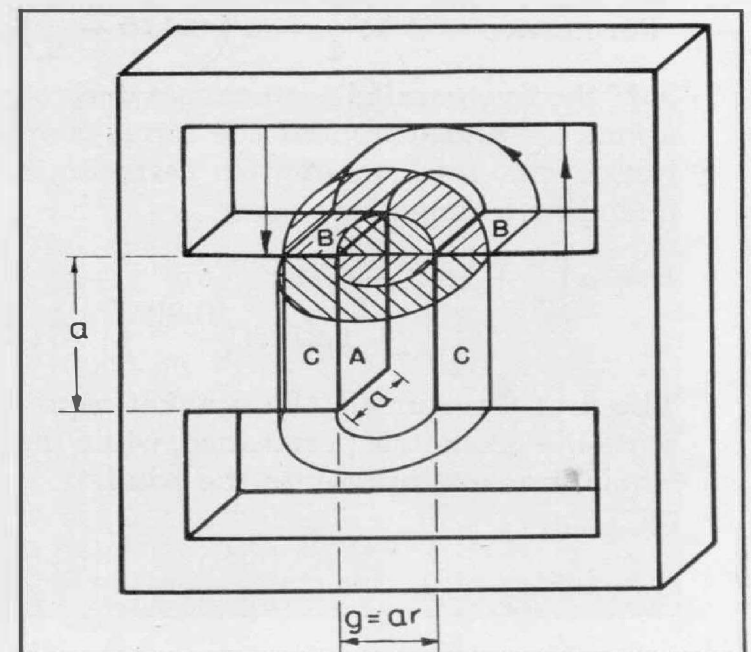
Roters' book. Figure 8 shows the types of simple-shaped volumes which can be used to calculate the permeance of the leakage field. Figure 17 illustrates the considerations which determine the radius of the extreme boundary of the leakage flux paths. The longest leakage flux line, following a semi-circular path, cannot be any longer than twice the height of the window, since the reluctance of the path for any longer leakage line would be less if the line merely jumped over to the adjacent outside leg and back again.

Figure 14 of this article shows the situation in and around the center-leg air gap for purposes of reference. Each of the two equal dimensions of the square cross section of the center leg is denoted by  $a$ . The air gap  $g$  is replaced by  $ar$  for convenience,  $r$  being the ratio of the air gap  $g$  to the tongue width  $a$ .

There are five different kinds of flux paths to be considered. Their number and permeances are as follows:

1. There is one geometric (non-leakage) flux path between the gap faces, a rectangular prism having a base area  $a^2$  and an altitude  $ar$ .

Figure 14. Fringing paths around a center-leg air gap.



$$\text{Permeance} = \frac{a^2}{ar} = \frac{a}{r}$$

2. There are four equal semi-circular cylindrical volumes of axial length  $a$  and diameter  $ar$ . (§53,1.)

$$\text{Permeance} = 4 \times 0.26a = 1.04a$$

3. There are four spherical quadrants having a diameter of  $ar$ . (§53,3.)

$$\text{Permeance} = 4 \times 0.077ar = 0.31ar$$

4. There are four half annuli having an inside diameter  $ar$ , a length  $a$ , and a thickness  $T$  given by  $[a(0.446 - r/2)]$ . (§53,2.)

$$\begin{aligned} \text{Permeance} &= 4 \times \frac{a}{\pi} \ln \left( 1 + \frac{2T}{ar} \right) \\ &= 1.27a \ln \frac{0.892}{r} \end{aligned}$$

The equation for  $T$  is obtained in this way. The length of the extreme semi-circular magnetic line is  $[\pi(T + ar/2)]$ . Twice the window height is typically  $1.4a$ , as can be discerned by examining the dimensions of various GR laminations as listed in Figure 1<sup>3</sup>. These two values must be equal:

$$\pi \left( T + \frac{ar}{2} \right) = 1.4a \quad (32)$$

$$\text{from which } T = a \left( 0.446 - \frac{r}{2} \right) \quad (33)$$

5. There are four quadrants of spherical shells having inside diameter  $ar$  and thickness  $[a(0.446 - r/2)]$ . (§53,4.)

$$\text{Permeance} = 4 \times \frac{T}{4} = a \left( 0.446 - \frac{r}{2} \right)$$

If the five parallel permeances derived above are added up and the terms combined, the total estimated permeance, including leakage flux, is:

$$P = a \left[ \frac{1}{r} + 1.49 - 0.19r + 1.27 \ln \left( \frac{0.89}{r} \right) \right] \quad (34)$$

The first term inside the bracket represents the geometric permeance, while the whole bracket represents the total. The

<sup>3</sup> See Part I.

quotient of the two (first term and whole bracket) gives the ratio between the effective gap length and the measured gap length.

$$\frac{\text{eff. gap}}{\text{meas. gap}} = \frac{1}{r} \left[ \frac{1}{r} + 1.49 - 0.19r + 1.27 \ln \left( \frac{0.89}{r} \right) \right] \quad (35)$$

By appropriate choice of different multiplying factors for the permeances listed in 1, 2, and 4, similar expressions can be obtained for the ratio of effective air gap to measured gap for other than square-center-leg cross sections. For 2 : 1 aspect ratio (stack twice as high as tongue width),

$$\frac{\text{eff. gap}}{\text{meas. gap}} = \frac{2}{r} \left[ \frac{2}{r} + 2.01 - 0.19r + 0.905 \ln \left( \frac{0.89}{r} \right) \right] \quad (36)$$

For  $\frac{1}{2} : 1$  aspect ratio (gaps in outside legs of square-center-leg stack). (Note that  $r$  is ratio of gap length to width of center leg or tongue.)

$$\frac{\text{eff. gap}}{\text{meas. gap}} = \frac{1}{2r} \quad (37)$$

$$\left[ \frac{1}{2r} + 1.23 - 0.19r + 0.953 \ln \left( \frac{0.89}{r} \right) \right]$$

The curves in Figure 15 include not only a center one of correction factors for a core having a square stack with a center-leg gap, but there is also an upper one labeled 2 : 1 (fringing has less effect) for a core having the center leg stacked twice as high as the tongue width and with a center-leg gap. There is likewise a lower curve labeled  $\frac{1}{2} : 1$  (fringing has more effect) which represents the condition existing with equal gaps in the outer legs of a core which is stacked to a height equal to the tongue width. This curve shows why air gaps in outer legs are less effective than one in the center leg, and that the disparity increases as the gap increases.



The curves in Figure 15 are universally applicable to any size of laminations having approximately these proportions, since they have been normalized, that is, since they are plotted against the ratio of air gap to tongue width. For purposes of fringing calculations, the ratio of air gap to path length has no significance.

Two other points should be noted about these curves. First, they are not directly applicable without refiguring to so-called scrapless laminations, since the window height in those is  $0.5a$ . Equation (33) will have to be different for scrapless lamination shapes, and it in turn causes changes in parts 4 and 5 of the permeance calculations.

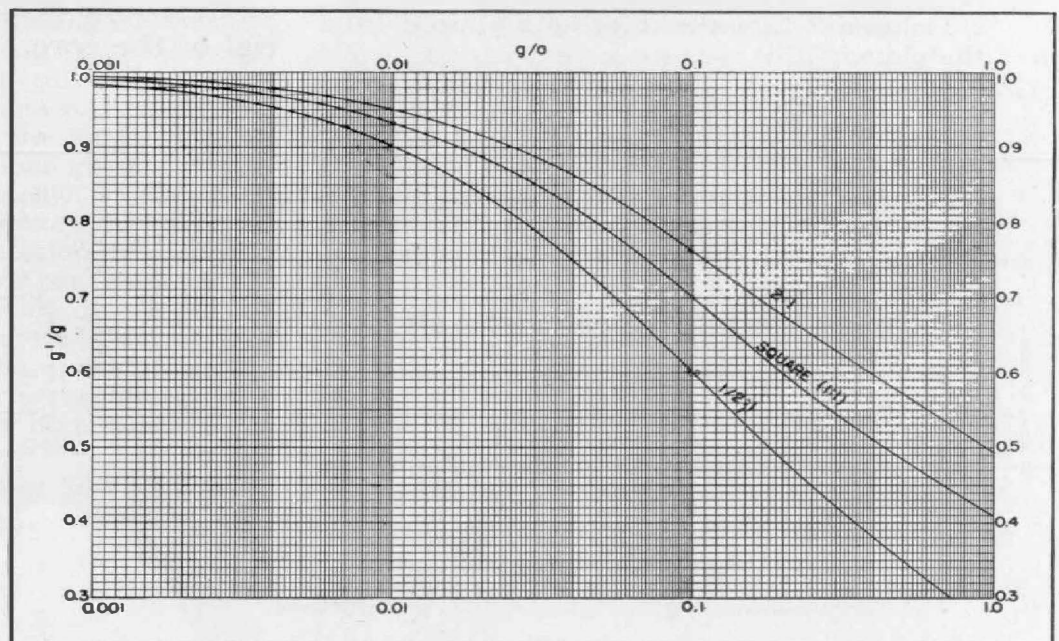
The other point is that this analysis is apparently too simple to hold strictly for very large gaps, as will be seen on the curves to be presented subsequently. Points for large gaps depart appreciably from the straight line. This is probably partly because Equation (33) has been used to determine all four of the half annular paths in 4 above, even though the (33) limitation is active only on two of them. Likewise the (33) limitation is active throughout only part of the permeance paths calculated under 5.

### Plotting the Straight Lines

Before the points representing individual measurements can be plotted to see how closely they lie on the  $45^\circ$  straight line of Equation (31), the data as recorded must be reworked.

To obtain the abscissa, each measured inductance must be divided into  $[4\pi N^2 A / 10^9]$ . In this expression,  $N$  is the number of turns in the coil, and  $A$  the area in square centimeters of the center-leg cross section. This quotient has the dimensions of a length in centimeters. Since it is desired that this length come out in mils, the value of the multiplier must be divided by 2.54 centimeters per inch, and

Figure 15. Ratio of effective to measured gap lengths as a function of the ratio  $g/a$ .



multiplied by 1000 mils per inch. Into this figure the values of inductance can then be divided.

To obtain the ordinate, the equivalent length  $g'$  of each air gap must be calculated by use of Figure 15. To use Figure 15, the ratio  $r [= g/a]$  is necessary to enter the chart on the axis of abscissae. The curve indicates, for the particular ratio, the correction factor which must be applied. The measured air gap in mils must be multiplied by this factor, the ordinate of the curve, to get the equivalent air gap  $g'$ . In the calculations for the 746 core, the upper curve in Figure 15 marked "2 : 1" should be used. For all the other laminations, the central curve marked "square" is the proper one.

Figures 16 through 19 show for each of the four lamination shapes the distribution of the corrected empirical points about the most probable  $45^\circ$  straight line through them. Where both A-metal and silicon-steel laminations of a given shape were measured, two different lines are plotted, sometimes to different scales, since the A-metal intercept is so small.

Several details should be observed about these plots.

A possible reason has already been advanced for the departure of the extreme right-hand point (large air gap) from the straight line.

The first point, at zero ordinate or butt joint, is often rather badly off the curve to the right. This is probably explainable on mechanical grounds, rather than as an error in measure-

ment. Sloping portions of center legs of most lamination shapes are half cut off in a kick press to eliminate any center leg interleaving. If these laminations are cut off just a little too much, then when they are completely interleaved into a coil, with the outer legs touching, the joint is not truly a butt joint, but has a finite gap length. This condition is not at all unlikely to occur. Corroboration of this view is given indirectly by the fact that the first or left-hand point for the 746 A-metal plot falls on the line very well. There happens to be for this lamination a special die with a square nose on the center leg (about which more will be said later), and with a center leg which was made slightly more than half as long as the outside leg, in order to be sure that a butt joint never had a finite length.

**Interpreting the Plots**

The first thing to be remarked in connection with the plots is the generally small departure of the points from the 45° lines, and the fairly random distribution of the sense of deviation. Plausible explanations have been proffered for the points which deviate worst.

The first conclusion, then, is that the calculations based on Roters truly represent the extent of fringing until the air gaps are quite large in proportion, say 3/10 of the tongue width.

The intercepts on the axis of ordinates should be interpreted to learn if possible what value should be assigned to the equivalent length of a butt joint. As pointed out earlier, the intercept represents a length which is equal to  $[b + (l/\mu_t\alpha)]$ . The quantity  $[l/\mu_t\alpha]$  is calculated for each lamination using a value of 0.96 for  $\alpha$ , and typical values for  $\mu_t$  of 470 for silicon steel and 2500 for A-metal. The table in Figure 20 lists the information deduced from the intercepts.

Column 1 lists lamination size and material.

Column 2 lists the intercepts as read from the plots.

Column 3 lists the calculated value of the equivalent air length of the ferro-magnetic material.

The length obtained by subtracting Column 3 from Column 2 is entered in the proper one of Columns 4, 5, and 6, depending on the shape of the nose on the center leg (see Figure 12 for contours). Flat-nose (Figure 12c) refers to a lamination which can be used only with an effective gap in the center leg and which has the end of the center leg perpendicular to its axis. The blunt-angled center leg (Figure 12a) is of the type where the sloping portion is not far angularly (about 13°) from the right-angled portion of the nose. The sharp-angled center leg (Figure 12b) has the sloping portion at an angle of 45°.

In the seventh column is listed the equivalent air length of the interleaved magnetic material as obtained from the measurement of inductance of the coil with fully interleaved, uncut laminations. This length can be compared with the typical calculated one in the third column. The value obtained from measurements (Column 7) will usually be seen to be larger than that obtained by calculation from ring-sample permeability value. This is because there is some reluctance in the interleaved joints which shows up as an increased effective air length. From this it may be seen that what has been called for convenience the equivalent length of a butt joint represents actually the equivalent length of a butt joint in series with parallel interleaved joints in the outside legs.

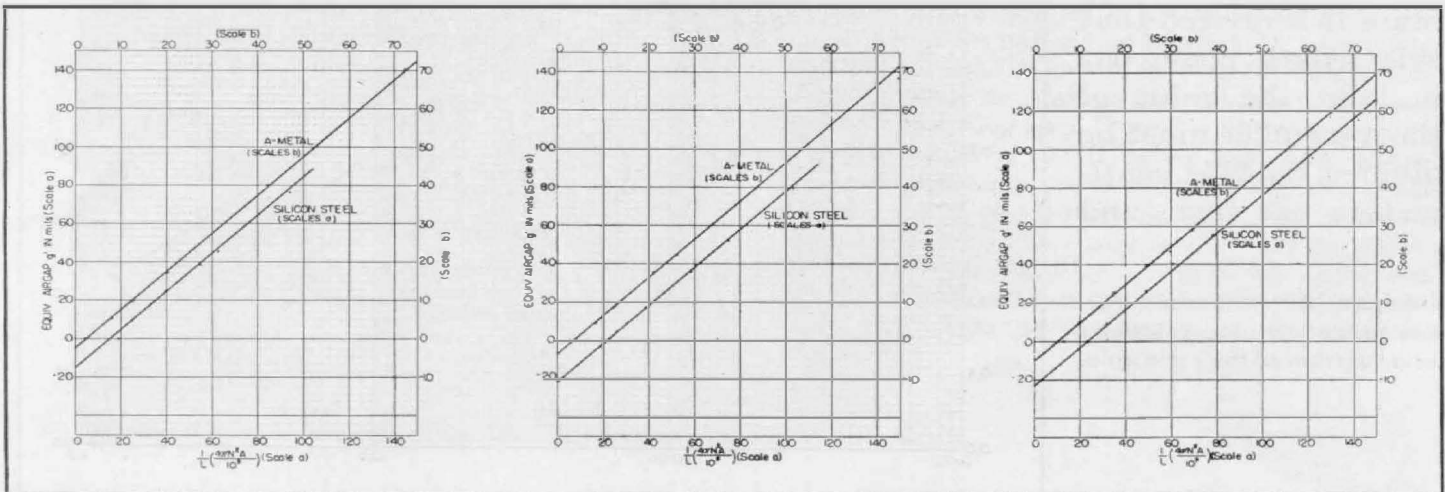
**Conclusions**

Some conclusions can be drawn from Figure 20. It appears that the effective length of a butt joint is a function both of the shape of the nose and of the material of the core.

Figure 16.

Figure 17.

Figure 18.



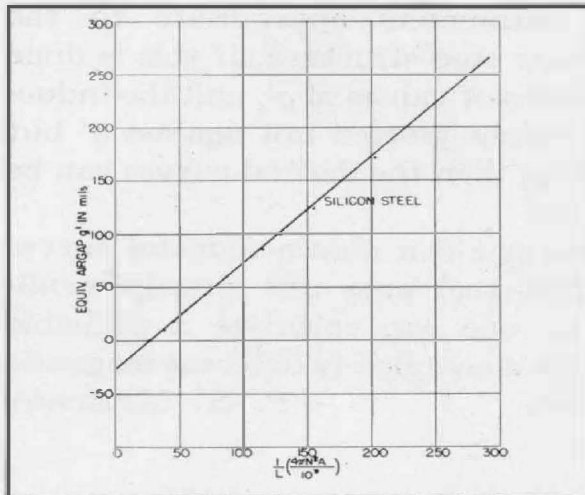


Figure 19.

1. For blunt-angle-nose silicon-steel laminations, the effective lengths come out as 9, 10, and 11 mils, and for sharp-angle-nose ones, one value of 10 mils was obtained. These are all of the same order of magnitude.

2. On the other hand, blunt-angle-nose A-metal laminations gave two values of  $b$  of about 5 and 8 mils.

3. The only flat-nose value, of 1.4 mils, came from measurements on A-metal laminations.

The marked difference between flat-nose and angle-nose effective  $b$ 's was at first surprising. After consideration of the conditions in the center-leg gap, the result was less surprising. Consider the conditions at the gap with angle-nose laminations. The flat portion of the end of each lamination comes opposite to the sloping portion of the end of its mating lamination. If there were only one pair of mating laminations in the core, the air gap would be quite large, since the laminations would truly butt at only one short line, not on a surface. Actually, of course, the interleaving of the laminations in successively opposite directions gives a double gridiron type of pattern on each cross-section face. The lines of force probably do not cross from straight to sloping portion of opposite laminations of a pair but, rather, go from the straight portion of a lamination on one side to the straight portions of the two laminations adjacent on each side to the opposite mating lamination. Whatever the true mechanism, the reluctance of the joint is very high compared to

Figure 12. Types of laminations: (a) blunt-angled; (b) sharp-angled; (c) flat.

LAMINATION SIZE & MAT'L	INTERCEPT mils	TYPICAL $\mu r$	EFFECTIVE LENGTH & FOR TYPE NOSE ON CENTER LEG			$\frac{1}{L} \left( \frac{4\pi N^2 A}{10^9} \right)$ FOR FULL INTERLEAVED CORE
			FLAT	BLUNT	SHARP	
746, AUDIO A	16	6	—	—	10	9.15
746, A-METAL	2.5	1.1	1.4	—	—	1.65
345, RT 72	21.7	10.7	—	11	—	13.2
345, A-METAL	7.2	2.0	—	5.2	—	2.1
485, RT 72	23.5	14.5	—	9	—	20.4
485, A-METAL	10.5	2.7	—	7.8	—	3.9
365, RT 72	28	18	—	10	—	17.5

Figure 20.

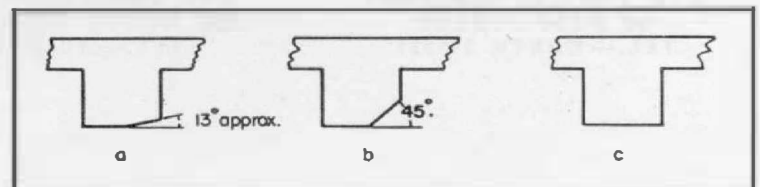
what can be obtained with properly designed flat-nose laminations. The fact that there is no sensible difference in  $b$  for the blunt- and the sharp-angle nose is some corroboration of the supposition that very few lines of force go from flat to mating sloping faces. Otherwise, there would be a noticeable difference in values of  $b$  for blunt and sharp angles, because of the great difference in average air gaps in the two cases.

The fact that the blunt-angle-nose A-metal laminations had lower  $b$ 's is not completely understood. It should be recognized that the method pursued is not inherently an accurate one. It involves measurements of inductance of coils on ferro-magnetic cores, which are sensitive to signal level and to mechanical treatment. These measurements have to be corrected by an approximate theory, an approximate line drawn through their plotted points, an intercept read graphically, and a calculated supposititious value for equivalent air length of the magnetic structure subtracted. All of the successive steps are subject to some error. It is perhaps surprising that the agreement is as good as it is, yet there may be some demonstrable reason for the  $b$  to be smaller with the higher-permeability material.

There is only one value for a flat-nose core. It agrees fairly well with a figure of around 1.5 mils, which was obtained from a completely independent type of measurement, using DC instead of AC. The value is believed to be reasonable.

### How to Use This Information

It is now possible to calculate with some fair expectation of accuracy a





curve similar to the second curves of Figures 2 to 11<sup>4</sup> for some other combination of lamination dimensions and material. The inductance can be calculated from Equation (31). The effective gap length  $g'$  in that equation can be obtained by use of the curves of Figure 15. The equivalent air length  $b$  of a butt joint can be obtained by judicious use of the information in Figure 20.  $[l/\mu_t\alpha]$  can be calculated from the values of the

three parameters appropriate to the particular core structure. If this is done for a series of values of  $g'$ , and the inductance values plotted not against  $g'$  but against  $g$ , then the desired curves can be obtained.

Thus, one can obtain A-metal curves if silicon-steel ones are already available, or one can calculate a probable curve for a completely different magnetic structure. — P. K. McELROY

<sup>4</sup> See Part I.

## F. C. C. APPROVAL NUMBERS FOR GENERAL RADIO BROADCAST MONITORS

After completion of type tests, the Federal Communications Commission has approved both the TYPE 1181-A Frequency Deviation Monitor and the

TYPE 1931-A Modulation Monitor and has granted the following approval numbers:

TYPE 1931-A Amplitude-Modulation Monitor — F.C.C. Approval No. 1555.  
TYPE 1181-A Frequency Deviation Monitor — F.C.C. Approval No. 1467.

## MISCELLANY

Visitors to our plant and laboratories in the last few months include Mr. F. S. Hewitt, Director, Tele-communications Research Laboratory, University of Witwatersrand, Johannesburg, South Africa; Mr. Olle Wernholm, Electronic Research Division, Royal Institute of Technology, Stockholm, Sweden; Professor Segismundo Gerszonowicz, Head of the Department of Electrical En-

gineering, University of Montevideo, Uruguay; Professor J. Oskar Nielsen, Royal Technical College, Copenhagen, Denmark; Mme. Nikis and M. G. H. Bezy, Les Laboratoires Radioelectriques, Paris, France; and Mr. V. A. Altovsky, Chief, High-Frequency Research Laboratory, Compagnie Francais Thomson-Houston, Paris.

### GENERAL RADIO COMPANY

275 MASSACHUSETTS AVENUE

CAMBRIDGE 39

MASSACHUSETTS

TELEPHONE: TROWBRIDGE 4400

### BRANCH ENGINEERING OFFICES

NEW YORK 6, NEW YORK  
90 WEST STREET  
TEL.—WORTH 2-5837

LOS ANGELES 38, CALIFORNIA  
950 NORTH HIGHLAND AVENUE  
TEL.—HOLLYWOOD 6201

CHICAGO 5, ILLINOIS  
920 SOUTH MICHIGAN AVENUE  
TEL.—WABASH 3820